J. Fluid Mech. (2006), *vol.* 562, *pp.* 173–182.
doi:10.1017/S0022112006001194 Printed in the United Kingdom

Flow and solute uptake in a twisting tube

By R. D. O'DEA AND S. L. WATERS

Division of Applied Mathematics, School of Mathematical Sciences, University of Nottingham, University Park, Nottingham, NG7 2RD, UK

(Received 19 January 2006 and in revised form 30 May 2006)

We investigate flow in a tube driven by axial and radial wall oscillations that are periodic in time. Furthermore, the walls undergo periodic circumferential oscillations, the amplitude of which increases with axial distance along the tube; this wall motion results in a new mechanism for the generation of axial flows within the tube. The axial steady-streaming flows that arise as a result of circumferential oscillations are opposed to those due to the axial and radial pulsations, and are potentially as significant. We then consider the uptake of a passive solute through the walls of such a tube into an adjacent medium in which the solute diffuses and is consumed at a constant rate. The tube ends are open to well-mixed fluid containing the solute. The effect of the streaming flows on the solute flux into the tube is determined. The solute disperses along the tube due to the interaction between advection and transverse diffusion, and the time-mean solute distribution throughout the tube is determined for a wide range of parameters.

1. Introduction

We consider the flow of a homogeneous incompressible Newtonian fluid within an axisymmetric tube whose wall is subject to radial and axial oscillations. In addition, the wall is subject to circumferential oscillations, the amplitude of which increases with axial distance along the tube. We focus attention on the steady-streaming flow that is induced by such wall motion. While the effect of radial and axial oscillations on the fluid flow has been studied (Secomb 1978; Waters 2004), the role of circumferential oscillations whose amplitude increases with axial distance along the tube, or *twist*, has not been considered. The circumferential wall motion leads to the generation of a circumferential fluid velocity which depends on the axial coordinate. To maintain this motion a fluid pressure is generated which depends on the axial coordinate, and the resulting axial pressure gradient thus drives flow along the vessel; this represents a new mechanism for the generation of axial flows within the tube. We show that the circumferential wall oscillations are potentially as significant as the radial and axial pulsations for the internal tube flow. This problem belongs to a broader class of steady-streaming problems, see for example Riley (1991), Riley & Wybrow (1995), Riley (2001) and references therein.

One example of fluid flow within tubes whose walls are subject to radial, axial and circumferential oscillations is coronary artery flow. The muscle fibres of the heart are so arranged as to result in a wringing type of movement that efficiently squeezes blood from the heart with each cardiac beat. The coronary arteries supply the heart muscle with nutrients and oxygen and remove metabolites and waste products. Many of these vessels penetrate the heart muscle itself and thus their overall geometry, represented by the vessel diameter and length, changes over time with each beat. Furthermore, they are themselves subject to a wringing motion with each cardiac beat. To date, the effect of this wringing motion on coronary artery blood flow and nutrient and metabolite transport has not been considered. Motivated by this application, we will also determine the influence of fluid flow on the delivery of a passive solute through the walls of the tube into a surrounding medium in which the solute diffuses and is consumed at a constant rate. We recognize that physiologically coronary artery flows are more complex than the flows considered here; as well as breaking axisymmetry, aspects such as the time-dependent driving axial pressure gradient and the time-dependent curvature of the artery should also be considered (Lynch, Waters & Pedley 1996; Waters & Pedley 1999; van Meerveld & Waters 2001). However, for simplicity, we restrict attention to the simplified model here to illustrate that circumferential wall oscillations can generate axial flows along the tube, hence motivating the inclusion of such effects in subsequent studies of arterial blood flow.

The fluid motion is driven entirely by the wall motion and is governed by the Navier–Stokes and continuity equations together with the no-slip boundary condition at the tube walls. The wall oscillations are sinusoidal in time, with dimensionless frequency parameter, α, and amplitude, ε. The phases of the axial and circumferential wall motions are assumed to differ from those of the radial motion by ψ and ϕ respectively. We consider two flow regimes corresponding to asymptotically small frequency ($\alpha \ll 1, \varepsilon = O(1)$) and asymptotically small amplitude ($\varepsilon \ll 1, \alpha = O(1)$). In coronary arteries, $\alpha \approx 1$ (Waters & Pedley 1999) so we consider the solute transport problem for the latter case. The solute transport is modelled by an advection–diffusion equation in the tube and a diffusion–consumption equation in the surrounding medium; these equations are coupled via the boundary conditions at the permeable tube walls. By considering a parameter expansion in powers of ε for the dependent variables we are able to determine the time-mean solute distribution. We consider solutes for which the molecular diffusivity is small, so that longitudinal diffusion is negligible and the dominant spreading mechanism for the solute in the tube is the interaction between advection and transverse diffusion (shear dispersion). The analysis will be restricted to the transport of solutes for which the Schmidt number, the ratio of kinematic viscosity to molecular diffusivity, is large, e.g. the Schmidt number for oxygen in blood is estimated to be $O(10^3)$ (Waters 2001).

When a passive solute is injected into fluid flowing along a tube or channel, it spreads out along the tube in the direction of the flow owing to longitudinal molecular diffusion and shear dispersion. The dispersion of a bolus of diffusing solute in a fluid flowing along a long rigid cylindrical impermeable tube was first studied by Taylor (1953) and Aris (1956). Taylor showed that the longitudinal spreading of the solute is enhanced by the non-uniformity of the velocity profile and limited by lateral mixing. A wide variety of dispersion problems have subsequently been studied; see, for example, Secomb (1978), Hydon & Pedley (1993), Waters (2001, 2004) and references therein. Here we show that the flow induced by the circumferential wall oscillations is potentially as significant as the radial and axial pulsations for solute dispersion and solute delivery to the adjacent medium.

In § 2 the problem is formulated mathematically and the governing equations for the fluid flow and solute concentration are given in §§ 2.1 and 2.2 respectively. In § 3.1 we give the similarity solution for fluid flow along the tube and in § 3.2 we solve the solute concentration equations subject to the appropriate boundary conditions. Finally in § 4 the implications of these results are discussed.

2. Formulation

We consider an axisymmetric tube surrounded by a radially infinite homogeneous medium; see figure 1. A cylindrical coordinate system (r^*, Φ, z^*) is chosen with

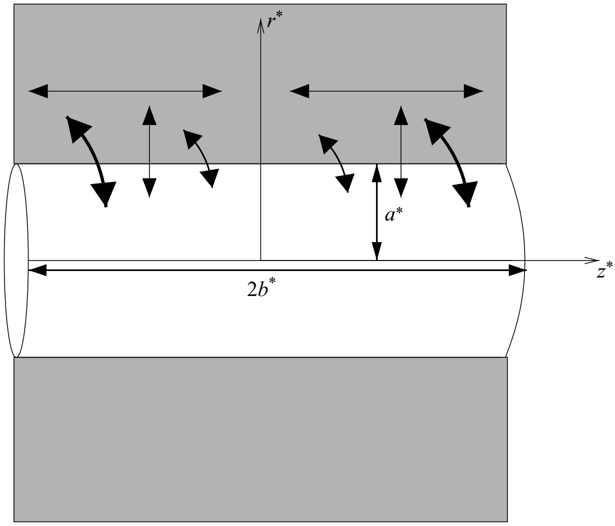

FIGURE 1. Definition sketch. We consider a long thin tube corresponding to $a^* \ll b^*$.

corresponding coordinate directions $(\hat{\boldsymbol{r}}, \hat{\boldsymbol{\Phi}}, \hat{\boldsymbol{z}})$. Throughout this paper, asterisks denote dimensional quantities. The fluid motion is driven entirely by the motion of the tube wall. The tube length, $2b^*(t^*)$, varies with time, t^*, and the tube walls move in the radial direction in a prescribed way, so that $r^* = a^*(t^*)$ at the tube–medium interface, where a^* is the tube radius. The variation of tube radius and length with time is assumed to be oscillatory (Waters 2001, 2004) so that

$$a^* = a_0^* a, \quad b^* = b_0^* b, \quad \text{where} \quad a(t^*) = 1 + \varepsilon \mathscr{A} \sin \omega^* t^*, \quad b(t^*) = 1 + \varepsilon \mathscr{B} \sin(\omega^* t^* + \psi). \tag{2.1}$$

The time-mean radius and length are a_0^*, b_0^* respectively, the amplitudes of the radial and axial oscillations are $\varepsilon a_0^* \mathscr{A}$ and $\varepsilon b_0^* \mathscr{B}$ respectively, ω^* is the angular frequency of oscillations and ψ is the phase difference between the two motions. The circumferential wall motion is also assumed to be oscillatory and, in addition, linearly increasing with the axial coordinate, z^*. Thus we impose that the circumferential tube wall velocity is $(\varepsilon V_w^* z^*/b^*) \cos(\omega^* t^* + \phi)$, where $\varepsilon V_w^* z^*/b^*$ is the amplitude of the motion and ϕ is the difference in phase between the circumferential and radial oscillations.

The tube contains an incompressible homogeneous viscous Newtonian fluid of kinematic viscosity, ν^*, and density, ρ^*, with velocity components, $\boldsymbol{u}^* = (u^*, v^*, w^*)$, and pressure, p^*. The open ends of the tube are exposed to a well-mixed fluid containing a solute at concentration C_0^*, and the solute concentrations in the tube and the surrounding medium are $C_0^* C$ and $C_0^* \theta$ respectively. The solute diffusivity, D^*, is assumed to take the same constant value in both the fluid and the medium. The medium consumes solute at a constant rate, Q^*. The interfacial wall is impermeable to fluid but allows the passage of solute with a permeability coefficient Π^*.

2.1. *Fluid flow*

The fluid flow is governed by the continuity and Navier–Stokes equations. It is convenient to choose a frame of reference in which the walls are fixed, and so following Secomb (1978) we non-dimensionalize as follows:

$$\left.\begin{aligned} r^* &= a^* r, \quad z^* = b^* z, \quad t^* = t/\omega^*, \\ u^* &= \omega^* a_0^* u, \quad (v^*, w^*) = \omega^* b_0^*(v, w), \quad p^* = \frac{\nu^* \rho^* \omega^* b_0^{*2}}{a_0^{*2}} p. \end{aligned}\right\} \tag{2.2}$$

Since we are considering a long thin tube with aspect ratio $\delta = a_0^*/b_0^* \ll 1$, the governing equations may be simplified by making the long-wavelength approximation. We therefore neglect terms of $O(\delta^2)$ in the governing equations. Seeking axisymmetric solutions $\boldsymbol{u} = \boldsymbol{u}(r, z, t)$, $p = p(r, z, t)$, the simplified dimensionless governing equations are: continuity, radial momentum

$$\frac{1}{r}\frac{\partial}{\partial r}(ru) + \frac{a}{b}\frac{\partial w}{\partial z} = 0, \qquad \frac{v^2}{r} = \frac{1}{\alpha^2}\frac{\partial p}{\partial r}, \tag{2.3a}$$

circumferential momentum

$$\frac{\partial v}{\partial t} + \left(\frac{u}{a} - \frac{\dot{a}}{a}r\right)\frac{\partial v}{\partial r} + \left(\frac{w}{b} - \frac{\dot{b}}{b}z\right)\frac{\partial v}{\partial z} + \frac{uv}{ar} = \frac{1}{a^2\alpha^2}\left[\frac{1}{r}\frac{\partial}{\partial r}\left(r\frac{\partial v}{\partial r}\right) - \frac{v}{r^2}\right], \tag{2.3b}$$

axial momentum

$$\frac{\partial w}{\partial t} + \left(\frac{u}{a} - \frac{\dot{a}}{a}r\right)\frac{\partial w}{\partial r} + \left(\frac{w}{b} - \frac{\dot{b}}{b}z\right)\frac{\partial w}{\partial z} = -\frac{1}{\alpha^2 b}\frac{\partial p}{\partial z} + \frac{1}{\alpha^2 a^2 r}\frac{\partial}{\partial r}\left(r\frac{\partial w}{\partial r}\right), \tag{2.3c}$$

where dots denote derivatives with respect to dimensionless time. The corresponding boundary conditions are

$$u = \dot{a}, \quad v = \frac{\varepsilon\beta z}{\alpha^2}\cos(t + \phi), \quad w = z\dot{b} \quad \text{at} \quad r = 1, \tag{2.4a}$$

$$u = 0, \quad v = 0, \quad w = \text{bounded} \quad \text{at} \quad r = 0. \tag{2.4b}$$

In addition to the dimensionless parameters ε, $\mathscr{A}$, $\mathscr{B}$, ψ and ϕ, the flow is parameterized by two further dimensionless parameters: $\beta = V_w^* a_0^{*2}/\nu^* b_0^*$, which characterizes the amplitude of the circumferential oscillations, and the Womersley parameter (or dimensionless frequency parameter), $\alpha = a_0^*(\omega^*/\nu^*)^{1/2}$, where α^2 is the ratio of the timescale for viscous diffusion of momentum to the period of oscillation.

2.2. *Solute concentration*

The dimensionless equations for the solute concentrations in the tube, C, and in the surrounding medium, θ, are respectively

$$\frac{\partial C}{\partial t} + \left(\frac{u}{a} - \frac{\dot{a}}{a}r\right)\frac{\partial C}{\partial r} + \left(\frac{w}{b} - \frac{\dot{b}}{b}z\right)\frac{\partial C}{\partial z} = \frac{1}{\sigma\alpha^2}\frac{1}{a^2 r}\frac{\partial}{\partial r}\left(r\frac{\partial C}{\partial r}\right), \tag{2.5}$$

$$\frac{\partial \theta}{\partial t} - \frac{\dot{a}}{a}r\frac{\partial \theta}{\partial r} - \frac{\dot{b}}{b}z\frac{\partial \theta}{\partial z} = \frac{1}{\sigma\alpha^2}\left[\frac{1}{a^2 r}\frac{\partial}{\partial r}\left(r\frac{\partial \theta}{\partial r}\right) - \lambda\theta\right], \tag{2.6}$$

where $\sigma = \nu^*/D^*$ is the Schmidt number, $\lambda = a_0^{*2}Q^*/D^*$ is the ratio of the diffusion and consumption timescales in the medium, and we again neglect terms of $O(\delta^2)$ so that the effects of longitudinal diffusion are neglected.

The boundary conditions are: (*a*) continuity of solute flux at the tube–medium interface (which allows a discontinuity in the solute concentration); (*b*) zero flux at the tube centreline; and (*c*) the solute concentration in the medium decays away from the tube walls in the radial direction. These are expressed as

$$\frac{k}{a}\frac{\partial C}{\partial r} = -(C - \theta) = \frac{k}{a}\frac{\partial \theta}{\partial r} \quad \text{at } r = 1, \quad \frac{\partial C}{\partial r} = 0 \quad \text{at } r = 0, \quad \theta \to 0 \quad \text{as } r \to \infty, \tag{2.7}$$

where $k = D^*/(a_0^* \Pi^*)$ is the ratio of the timescales of uptake to diffusion. At $z = 1$, we assume that $C = 1$ and we assume the concentration in the medium adjusts accordingly (see Waters (2001) for a full discussion of this boundary condition). At $z = 0$ we assume that the concentration profile is symmetric so that $\partial C/\partial z = \partial\theta/\partial z = 0$ there.

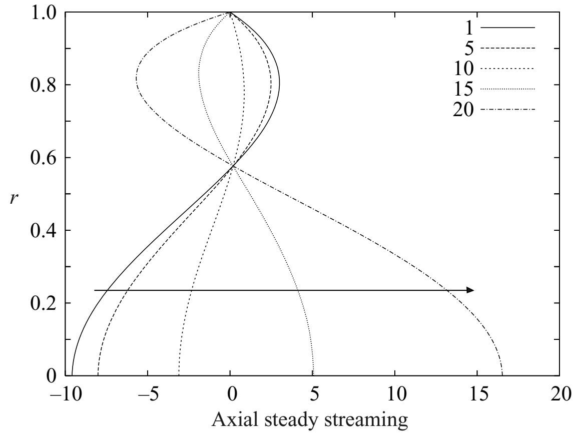

FIGURE 2. Axial steady streaming as a function of radius r for $\hat{\beta}=1, 5, \ldots, 20$. The arrow indicates the direction of increasing $\hat{\beta}$. The tube wall is at $r=1$ and the centreline at $r=0$. $\mathscr{A}=\mathscr{B}=1$, $\phi=\psi=0$.

3. Solution

3.1. *Fluid flow*

Motivated by the form of the boundary conditions (2.4) and inspection of the governing equations (2.3), we seek a similarity solution of the form

$$(u, v, w, p) = (aU, zV, zbW, P_0 + z^2 P), \tag{3.1}$$

where the functions U, V, W, P are independent of z and P_0 is constant. Note that this similarity solution will not be valid at a dimensionless distance of $O(\delta)$ from the tube ends. We now consider two flow regimes corresponding to $\alpha \ll 1$, $\varepsilon = O(1)$ and $\alpha = O(1)$, $\varepsilon \ll 1$ respectively.

3.1.1. *Solution for small* α

We start by considering the amplitude of the wall oscillations to be $O(1)$ and the Womersley parameter to be small. We expand the dependent variables in powers of α as $U = U_0 + \alpha^2 U_1 + \cdots$, with similar expansions for V, W and P. In order that the circumferential motions remain $O(1)$ as $\alpha^2 \to 0$ we assume that $\beta = \alpha^2 \hat{\beta}$. We find that

$$U = -\frac{a^2 P_0}{2b^2}\left(\frac{r^3}{4} - \frac{r}{2}\right) - \frac{\dot{b}r}{2b} + O(\alpha^2),\ V = \varepsilon\hat{\beta} r\cos(t+\phi) + O(\alpha^2), \tag{3.2a}$$

$$W = \frac{a^2 P_0}{2b^2}(r^2-1) + \frac{\dot{b}}{b} + \alpha^2\left[\frac{a^2}{352}\left(\frac{a^2 P_0}{b^2}\right)^2 (4r^6 - 27r^4 + 30r^2 - 7)\right.$$
$$\left. + \frac{1}{48}\left(\frac{a^2\varepsilon^2\hat{\beta}^2}{b^2}\cos^2(t+\phi) + \frac{a^2}{b}\frac{d}{dt}\left(\frac{a^2 P_0}{2b}\right) + \frac{a^2 P_0 \dot{b}}{2b^3}\right)(3r^2-1)(r^2-1)\right] + O(\alpha^4), \tag{3.2b}$$

where P_0 is the leading-order pressure given by

$$P_0 = \frac{8b^2}{a^2}\left(\frac{\dot{a}}{a} + \frac{\dot{b}}{2b}\right). \tag{3.3}$$

The axial steady streaming is determined by integrating the $O(\alpha^2)$ terms in equation (3.2b) over one period. In figure 2, the axial steady streaming is plotted as a function of r for several values of the twist parameter, $\hat{\beta}$. We remark that, for simplicity, we have set the phase differences ϕ, ψ to zero. As $\hat{\beta}$ increases, the flow direction reverses, changing from having the properties of flow driven by radial and axial oscillations only (i.e. flow in the direction of $z=0$ in the centre of the tube) to flow driven by circumferential oscillations only (flow in the direction of increasing z in the centre of the tube). The critical value of $\hat{\beta}$ at which this change occurs is between 10 and 15; however, we do not determine this value since we are interested in demonstrating the qualitative behaviour of the flow only. We remark that the point at which the the steady streaming passes through zero is $r \approx 1/\sqrt{3}$. This may be seen from inspection of the $O(\alpha^2)$ terms in equation (3.2b) whose (relevant) roots are $r = 1/2(23/2 - \sqrt{417}/2)^{1/2}$ and $1/\sqrt{3}$ respectively.

3.1.2. *Solution for small wall displacements*

The amplitude of the tube wall oscillations is assumed to be small ($\varepsilon \ll 1$) and we consider a small-parameter expansion of the dependent variables of the form

$$U(r,t) = \varepsilon\left[U^{[11]}(r)\mathrm{e}^{\mathrm{i}t} + \text{c.c.}\right] + \varepsilon^2\left[(U^{[20]}(r) + \text{c.c.}) + (U^{[22]}(r)\mathrm{e}^{2\mathrm{i}t} + \text{c.c.})\right] + \cdots, \quad (3.4)$$

where c.c. denotes the complex conjugate. Similar expansions are used for the solutions V, W, P. The functions $U^{[ij]}$ represent the jth Fourier coefficient of the ith-order term in the expansion of U. The time-independent terms of $O(\varepsilon^2)$ represent the steady streaming resulting from the convective inertia terms. Since the steady-streaming Reynolds number, $R_s = \varepsilon^2\alpha^2$ is small, we carry out a uniform series expansion of the governing equations (2.3) by considering successive orders of ε. To determine the leading-order time-mean solute distribution, we require explicit expressions for the leading-order solutions $W^{[11]}$, $U^{[11]}$, $V^{[11]}$, $P^{[11]}$ and the axial steady streaming, $W^{[20]}$, which are found to be

$$W^{[11]} = \frac{1}{4E}\left(2\mathscr{A}[I_0(\gamma r) - I_0(\gamma)] + \widetilde{\mathscr{B}}\left[I_0(\gamma r) - \frac{2}{\gamma}I_1(\gamma)\right]\right), \quad (3.5a)$$

$$U^{[11]} = \frac{1}{4E}\left(\mathscr{A}\left[I_0(\gamma)r - \frac{2}{\gamma}I_1(\gamma r)\right] + \widetilde{\mathscr{B}}\left[\frac{1}{\gamma}I_1(\gamma)r - \frac{1}{\gamma}I_1(\gamma r)\right]\right), \quad (3.5b)$$

$$V^{[11]} = \frac{\widetilde{\beta} I_1(\gamma r)}{2\alpha^2 I_1(\gamma)}, \qquad P^{[11]} = \frac{1}{4E}[\mathscr{A}\gamma^2 I_0(\gamma) + \widetilde{\mathscr{B}}\gamma I_1(\gamma)], \quad (3.5c)$$

$$\begin{aligned} W^{[20]} = \frac{1}{16EE'}\Bigg[&\mathscr{C}\mathscr{C}' I_1(\gamma)(rI_1(\gamma' r) - I_1(\gamma')) - 6\mathrm{i}\mathscr{C}'\left(\mathscr{A}I_0(\gamma) + \frac{\widetilde{\mathscr{B}}}{\gamma}I_1(\gamma)\right)(I_0(\gamma' r) - I_0(\gamma')) \\ &+ \Bigg\{12\mathrm{i}\mathscr{A}\mathscr{C}' I_0(\gamma)I_0(\gamma') - \left(\frac{24\mathrm{i}\widetilde{\mathscr{B}}\mathscr{C}'}{\gamma\gamma'} + 3\mathscr{C}\mathscr{C}'\right)I_1(\gamma)I_1(\gamma') + 4\int_0^1 r\mathscr{W}(r)\,\mathrm{d}r \\ &+ (16\mathscr{C}\mathscr{C}' + 24\mathscr{A}(\widetilde{\mathscr{B}}' - \widetilde{\mathscr{B}}))\frac{I_0(\gamma)I_1(\gamma')}{\gamma}\Bigg\}(r^2 - 1) \\ &- \mathrm{i}\gamma\mathscr{C}\mathscr{C}'\int_1^r I_1(\gamma r)I_0(\gamma' r)\,\mathrm{d}r + \mathscr{W}(r)\Bigg], \end{aligned} \quad (3.5d)$$

where $\mathscr{C} = 2\mathscr{A} + \widetilde{\mathscr{B}}$, $\widetilde{\mathscr{B}} = \mathscr{B}\mathrm{e}^{\mathrm{i}\psi}$, $\widetilde{\beta} = \beta\mathrm{e}^{\mathrm{i}\phi}$, I_0, I_1 are modified Bessel functions of the first kind of zeroth and first order respectively, $\gamma = \alpha\mathrm{e}^{\mathrm{i}\pi/4}$, $E = I_0(\gamma)/2 - I_1(\gamma)/\gamma$ and primes denote complex conjugates of a variable or parameter. In equation (3.5d)

$$\mathscr{W}(r) = \frac{8EE'\beta^2}{\alpha^2 I_1(\gamma)I_1(\gamma')}\int_1^r \frac{1}{\tau}\int_0^\tau t\int_0^t \frac{I_1(\gamma r)I_1(\gamma' r)}{r}\,\mathrm{d}r\,\mathrm{d}t\,\mathrm{d}\tau. \quad (3.6)$$

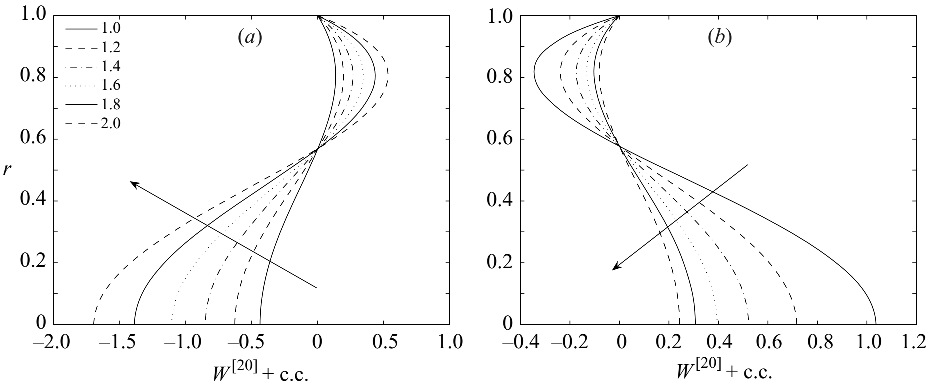

FIGURE 3. Axial steady streaming $W^{[20]}$ + c.c. as a function of radius r for $\alpha = 1, 1.2, \ldots, 2$. The arrow indicates the direction of increasing α. The tube wall is at $r = 1$ and the centreline at $r = 0$. (a) No twist ($\beta = 0$, $\mathscr{A} = \mathscr{B} = 1$). ($b$) Twist only ($\beta = 10$, $\mathscr{A} = \mathscr{B} = 0$).

Note that we need not compute the steady-streaming radial and circumferential velocities here as they are not required in the subsequent analysis.

In figure 3 the axial steady streaming $W^{[20]}$ + c.c. is plotted as a function of r for several values of α. In these figures we set $\phi = \psi = 0$. In figure 3(a), in which there is no circumferential wall motion, the flow is in the direction of increasing z close to the tube walls and is towards $z = 0$ in the centre of the tube. As α increases the amplitude of the velocity profile increases. The opposite is true when the wall motion only undergoes circumferential oscillations; see figure 3(b) where the flow is in the direction of increasing z in the centre of the tube, towards $z = 0$ close to the tube walls, and the amplitude of the velocity profile decreases as α increases. This is a consequence of the boundary condition for v given in (2.4a) which indicates that as α increases, the amplitude of the prescribed circumferential wall oscillations decreases. When flow is driven by axial, radial and circumferential oscillations, we find that, similarly to the $\alpha \ll 1$ regime, a critical value of β exists at which the velocity profile changes from having the properties of flow driven by radial and axial oscillations only to flow driven by circumferential oscillations only; the flow profile is qualitatively identical to that shown in figure 2.

We remark here that the steady streaming is unaffected by the presence of the circumferential phase difference, ϕ, since its influence is only felt through the combination $V^{[11]}V^{[11]'}$. The dependence of the axial steady streaming on ψ is such that as ψ increases between 0 and π the axial flow arising as a result of radial and axial pulsations retains the profile shape shown in figure 3(a), but the amplitude decreases. Upon increasing ψ from π to 2π the amplitude then increases (results not shown).

3.1.3. *Steady-streaming mechanism*

In both parameter regimes, the mechanism for generating axial steady-streaming flows is as follows. The amplitude of the circumferential wall oscillations is assumed to be a linear function of the axial coordinate, z. This wall motion leads to the generation of a circumferential fluid velocity that depends on z. To maintain this fluid motion a fluid pressure is generated which also depends on z, and the resulting axial pressure gradient then drives flow along the tube. We note that in both regimes considered, the leading-order circumferential fluid velocity is an increasing function of r (see (3.2a) and (3.5c)). Thus, the magnitude of the resulting steady axial pressure gradient will be largest near the tube wall. Furthermore, the pressure gradient will be positive. Thus steady axial flow will be driven towards $z=0$ near the tube walls, and conservation of mass then demands that flow will be in the direction of increasing z in the centre of the tube. For the case of flows driven by radial and axial oscillations, we note that the resulting steady axial pressure gradient will be largest at the centre of the tube (where, for example, the leading-order axial fluid velocity relative to the axial wall velocity is largest) so that steady axial flows will be driven towards $z=0$ in the centre of the tube, with conservation of mass demanding that flow will be in the direction of increasing z near the tube walls.

3.2. *Solute concentration*

In the coronary arteries, $\alpha \approx 1$ (§ 1). Motivated by this, we determine the influence of the fluid flow ($\varepsilon \ll 1$, $\alpha = O(1)$ regime) on the solute delivery. To determine the leading-order time-mean governing equations for the solute concentrations in the tube and the medium we expand C and θ as follows (see Waters (2004) for further details):

$$C(r,z,t) = \mathscr{C}(r,z) + \varepsilon\left[C^{[11]}(r,z)\mathrm{e}^{\mathrm{i}t} + \mathrm{c.c.}\right] + O(\varepsilon^2), \tag{3.7a}$$

$$\theta(r,z,t) = \Theta(r,z) + \varepsilon\left[\theta^{[11]}(r,z)\mathrm{e}^{\mathrm{i}t} + \mathrm{c.c.}\right] + O(\varepsilon^2). \tag{3.7b}$$

Substitution of (3.7) into equations (2.5) and (2.6) yields the following equations for the leading-order concentrations $\mathscr{C}$, Θ:

$$\widetilde{U}\frac{\partial \mathscr{C}}{\partial r} + z\widetilde{W}\frac{\partial \mathscr{C}}{\partial z} = \frac{1}{\widetilde{P}r}\frac{\partial}{\partial r}\left(r\frac{\partial \mathscr{C}}{\partial r}\right), \tag{3.8a}$$

$$\frac{1}{r}\frac{\partial}{\partial r}\left(r\frac{\partial \Theta}{\partial r}\right) - \lambda\Theta = 0, \tag{3.8b}$$

where $\widetilde{P} = \alpha^2\sigma\varepsilon^2$, $\widetilde{U} = U^{[20]} - \mathrm{i}(U_r^{[11]'} - \mathscr{A}/2)(U^{[11]} - r\mathscr{A}/2) + \mathrm{c.c.}$, $\widetilde{W} = W^{[20]} - \mathrm{i}W_r^{[11]'}(U^{[11]} - r\mathscr{A}/2) + \mathrm{c.c.}$ and the r subscripts denote differentiation with respect to r. We note here that the velocities $\widetilde{\mathscr{U}}$ and $\widetilde{\mathscr{W}}$ are functions of the steady-streaming velocities $U^{[20]}$ and $W^{[20]}$, and combinations of the leading-order velocities $U^{[11]}$ and $W^{[11]}$. Since the leading-order velocities do not depend on the parameter, β, in the case of flows driven only by circumferential oscillations of the tube wall, $\widetilde{\mathscr{W}}$ and $\widetilde{\mathscr{U}}$ are identical to $W^{[20]}$ and $U^{[20]}$ respectively. Furthermore, the terms dependent on the leading-order velocities are small in the parameter regimes that we consider, so that in general $\widetilde{\mathscr{W}}$ and $\widetilde{\mathscr{U}}$ are qualitatively similar to $W^{[20]}$ and $U^{[20]}$ respectively, and we do not present separate plots.

The radial diffusion term enters the governing equation (3.8*a*) at this order provided that $\varepsilon \ll \widetilde{P} \ll \varepsilon^{-1}$. Equation (3.8*b*) has solution $\Theta = A(z)K_0(\sqrt{\lambda}r)$, where K_0 is the modified Bessel function of the second kind of order zero. The function $A(z)$ is dependent upon $\mathscr{C}(1,z)$ and is determined from the boundary condition (2.7). Following Waters (2004), we assume that $\varepsilon \ll \widetilde{P} \ll 1$ and decompose $\mathscr{C}$ into an averaged, r-independent part and a small fluctuation so that $\mathscr{C}(r,z) = \widehat{\mathscr{C}}(z) + \widetilde{P}\mathscr{C}^{(1)}(r,z)$, where the averaging operator is defined $\widehat{f} = 2\int_0^1 fr\,\mathrm{d}r$ and $\widehat{\mathscr{C}}^{(1)} \equiv 0$ by definition. We note that the term $\widetilde{P}\mathscr{C}^{(1)}$ includes terms of all orders $\geqslant 1$ in $\widetilde{P}$. Cross-sectional averaging then yields the following governing equation for $\widehat{\mathscr{C}}$:

$$z^2\frac{\mathrm{d}^2\widehat{\mathscr{C}}}{\mathrm{d}z^2} + 2z\frac{\mathrm{d}\widehat{\mathscr{C}}}{\mathrm{d}z} - \kappa\widehat{\mathscr{C}} = 0, \tag{3.9}$$

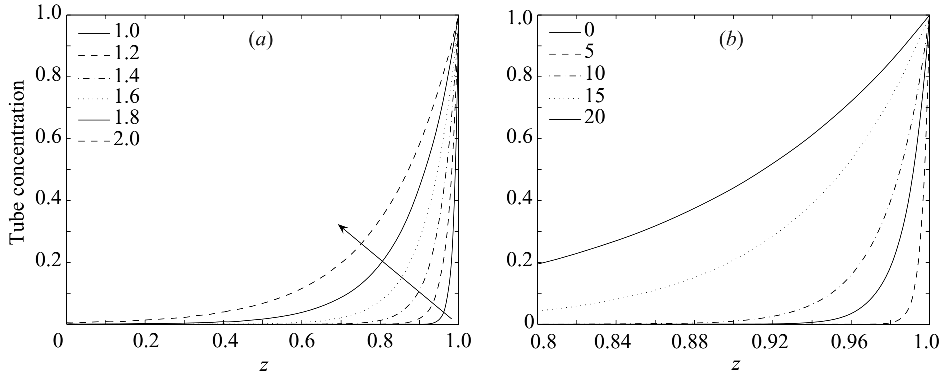

FIGURE 4. Solute concentration in the tube $\widehat{\mathscr{C}}$ as a function of axial position z. In all cases $\sigma = 10^3$, $\varepsilon = 10^{-2}$, $\varDelta = 0.2$, $\psi = \phi = 0$. (*a*) No twist ($\beta = 0$, $\mathscr{A} = \mathscr{B} = 1$). Here $\alpha = 1, 1.2, \ldots, 2$, and the arrow indicates the direction of increasing α. (*b*) With twist ($\alpha = \mathscr{A} = \mathscr{B} = 1$ and $\beta = 0, 5, \ldots, 20$).

where

$$\kappa = \frac{\varDelta}{\widetilde{P}^2} \frac{1}{\displaystyle\int_0^1 \mathscr{F}^2 r \, \mathrm{d}r}, \quad \mathscr{F} = \frac{1}{r} \int_0^r \widetilde{W} r \, \mathrm{d}r \quad \text{and} \quad \varDelta = \frac{\sqrt{\lambda} K_1(\sqrt{\lambda})}{K_0(\sqrt{\lambda}) + k\sqrt{\lambda} K_1(\sqrt{\lambda})}. \tag{3.10}$$

Following Waters (2001) we consider the limit in which $\kappa \gg 1$. We thus expect $\widehat{\mathscr{C}} \equiv 0$ except at small distances from the tube entrance. To determine the solute distribution in this region, we introduce a stretched coordinate, $\widehat{X}$, such that $1 - z = \widehat{X} \kappa^{-1/2}$. Equation (3.9) then reduces, at leading order, to $\widehat{\mathscr{C}}_{\widehat{X}\widehat{X}} - \widehat{\mathscr{C}} = 0$, the solution of which, satisfying $\widehat{\mathscr{C}}(1) = 1$ and $\widehat{\mathscr{C}}(\infty) = 0$ is, in original variables

$$\widehat{\mathscr{C}} = \exp\left\{ -\frac{\varDelta}{\widetilde{P}} \frac{1}{\sqrt{\displaystyle\int_0^1 \mathscr{F}^2 r \, \mathrm{d}r}} (1 - z) \right\}. \tag{3.11}$$

In figure 4(*a*) the time-mean solute concentration in a tube whose walls undergo radial and axial oscillations only is plotted as a function of z for several values of the frequency parameter α. The concentration of solute at a given z increases, corresponding to an increase in the solute flux into the tube as α increases. Furthermore, the solute penetrates further into the tube, due to the increased effects of shear dispersion; it is clear from figure 3(*a*) that the amplitude of the velocity profile increases as α increases. When the fluid flow is driven by circumferential oscillations of the tube wall only, we see that as α increases, both the amount of solute drawn into the tube and the degree of solute dispersion decrease (results not shown). This corresponds to the fact that as α increases, the amplitude of the velocity profile decreases so that the effects of shear dispersion are reduced; see figure 3(*b*). Finally we consider the case where the flow is driven by radial, axial and circumferential oscillations and vary β. The time-mean tube solute concentration in this case is plotted in figure 4(*b*). As β increases from zero we first see a decrease in solute flux and penetration. This corresponds to the initial decrease in the amplitude of the velocity profile as β increases from zero; see figure 2. However, as β increases further, and the amplitude of the corresponding velocity profile increases, the solute flux and penetration again increase, as expected.

4. Discussion

In this paper we have considered flow in an axisymmetric tube surrounded by a homogeneous medium. Flow in the tube is driven by a combination of radial, axial and circumferential oscillations. We have shown that these oscillations generate steady-streaming flows which enhance the flux of solute into the open ends of the tube, and the dispersion of solute along the tube. The solute disperses along the tube due to the interaction between longitudinal advection and transverse diffusion.

The consideration of circumferential wall oscillations has lead to the identification of a new mechanism by which axial flows can be generated along the tube. The amplitude of the circumferential wall oscillations is assumed to be a linear function of the axial coordinate, z, leading to the generation of a circumferential fluid velocity and pressure that depends on z. The resulting axial pressure gradient then drives flow along the tube. We note that this new mechanism for the generation of mean axial flows along a tube will hold for the amplitude of the wall oscillations being any arbitrary function of z; for simplicity we focused on a linear function of z here. The flows generated by circumferential oscillations of the tube wall are potentially as significant as those generated due to time-dependent variations in the tube volume (due to radial and axial wall oscillations) in determining the flow and subsequent solute distribution within the tube.

REFERENCES

Aris, R. 1956 On the dispersion of a solute in a fluid flowing through a tube. *Proc. R. Soc. Lond.* A **249**, 67–77.

Hydon, P. E. & Pedley, T. J. 1993 Axial dispersion in a channel with oscillating walls. *J. Fluid. Mech.* **249**, 535–555.

Lynch, D. G., Waters, S. L. & Pedley, T. J. 1996 Flow in a tube with non-uniform time-dependent curvature: governing equations and simple examples. *J. Fluid. Mech.* **323**, 237–265.

van Meerveld, J. & Waters, S. L. 2001 Numerical computation of the steady secondary flow in a tube with time-dependent curvature. *Q. J. Mech. Appl. Maths* **54**, 631–640.

Riley, N. 1991 Oscillating viscous flows: II superposed oscillations. *Mathematika* **38** (76), 203–216.

Riley, N. 2001 Steady streaming. *Annu. Rev. Fluid Mech.* **33**, 43–65.

Riley, N. & Wybrow, M. F. 1995 The flow induced by the torsional oscillations of an elliptic cylinder. *J. Fluid Mech.* **290**, 279–298.

Secomb, T. W. 1978 Flow in a channel with pulsating walls. *J. Fluid Mech.* **88**, 273–288.

Taylor, G. I. 1953 Dispersion of soluble matter in solvent flowing slowly through a tube. *Proc. R. Soc. Lond.* A **219**, 186–203.

Waters, S. L. 2001 Solute uptake through the walls of a pulsating channel. *J. Fluid Mech.* **433**, 193–208.

Waters, S. L. 2004 A mathematical model for the laser treatment of heart disease. *J. Biomech.* **37**, 281–288.

Waters, S. L. & Pedley, T. J. 1999 Oscillatory flow in a tube of time-dependent curvature. Part 1. Perturbation to flow in a stationary curved tube. *J. Fluid Mech.* **383**, 327–352.